

# INFLUENCE OF THE QUADRUPOLE PAIRING INTERACTION ON THE MEAN-SQUARE RADII OF NUCLEI\*

Z. LOJEWSKI, B. NERLO-POMORSKA AND K. POMORSKI

Institute of Physics, M. Curie-Skłodowska University  
pl. M. Curie-Skłodowskiej 1, Lublin, Poland

*(Received December 16, 1993)*

Microscopic static calculations of the mean-square charge radii of even nuclei are presented. It is shown that the quadrupole pairing forces influence the magnitude of the isotopic shift of  $\langle r^2 \rangle$ . The experimental data are better reproduced with quadrupole pairing interaction than with the monopole pairing only.

PACS numbers: 21.10. -k

## 1. Introduction

The use of laser techniques for the measurement of nuclear mean-square charge radii (msr) has resulted in a wealth of new information concerning this fundamental property of nuclei [1–4]. In recent years a number of theoretical papers have been devoted to estimate of isotopic shifts of the  $\langle r^2 \rangle$  of nuclei. In papers [5, 6], the ground-state static electric quadrupole and hexadecapole moments and mean-square radii of even nuclei were calculated microscopically.

The later papers [7–9] on the mean-square radii of nuclei have been based on the microscopic collective dynamical model and Nilsson single particle potential with the new universal set of parameters [10]. In [11] it is shown that isotopic shifts of mean square radii are well reproduced when omitting the isotopic factor in the oscillator frequency  $\hbar\omega_0$  in the Nilsson potential.

The aim of the present investigation is the analysis of the influence of the quadrupole pairing forces on the value of the mean-square radii of

---

\* Work supported partly by KBN, Project No. 203119101.

nuclei. As it was reported twenty years ago [12] the quadrupole pairing interaction plays an essential role in explaining the observed large change in  $\langle r^2 \rangle$  for neutron deficient Hg-isotopes. The model used in the present paper is similar to that described in Ref. [11]. Our calculations differ from those in [11] in the following points:

- we use the quadrupole pairing interaction;
- we use for simplicity the microscopic static model only.

The microscopic static calculation of the mean-square radii of nuclei follows in two steps. The first is the calculation of the equilibrium deformation of a nucleus and the other is the calculation of the msr for this given deformation. The first step involves finding the minimum of the potential energy treated as a function of the deformation. The second one aims at finding the wave function of a nucleus at the equilibrium point to calculate the average value of the corresponding multipole moment operator. We believe that including the quadrupole pairing interaction explains the discrepancy between experiment and theory.

## 2. Theoretical model

The calculations were performed for even-even isotopes in the range  $38 \leq Z \leq 78$  and  $Z \leq N \leq 120$ , *i.e.* Sr–Pt nuclei. The quadrupole  $\epsilon_2$  and hexadecapole  $\epsilon_4$  deformations were taken into account. In our model the many body Hamiltonian  $\hat{H}$  consists of the mean-field  $\hat{H}_0$  and the monopole and quadrupole pairing forces:

$$\hat{H} = \hat{H}_0 - G_0 P_0^\dagger P_0 - G_2 P_2^\dagger P_2. \quad (1)$$

The deformed single particle Nilsson potential with the universal set of parameters proposed by Seo [10] was used as the mean-field single particle Hamiltonian. The second and the third terms describe the monopole and quadrupole pairing residual interaction, respectively. Operators  $P_\lambda$  in (1) are defined as follows:

$$P_0^\dagger = \sum_{\nu} a_{\nu}^\dagger a_{\bar{\nu}}^\dagger, \quad (2)$$

$$P_2^\dagger = \sum_{\nu} q_{\nu\nu} a_{\nu}^\dagger a_{\bar{\nu}}^\dagger, \quad (3)$$

where  $q_{\nu\nu}$  are the single particle quadrupole moments. The strengths of the monopole  $G_0$  and quadrupole  $G_2$  pairing forces are taken from Ref. [12].

The ground state energy of a nucleus was evaluated [13] within the Strutinsky prescription. The energy of a nucleus consists of the macroscopic

liquid droplet  $E_{\text{LDt}}$  [14] part and the shell correction  $\Delta E_{\text{shell}}$  describing the shell and pairing effects.

$$\langle BCS | \hat{H} | BCS \rangle = E_{\text{LDt}} + \Delta E_{\text{shell}}. \quad (4)$$

The minimum of the energy (4) gives the equilibrium deformation parameters ( $\epsilon_2, \epsilon_4$ ).

The formulae for electric microscopic multipole moments  $Q_\lambda$ , calculated as the mean values of the  $\hat{Q}_\lambda$  operators in the ground-state  $BCS$  wave function are:

$$Q_\lambda = \sum_\nu q_{\nu\nu}^\lambda 2 v_\nu^2, \quad (5)$$

where  $q_{\nu\nu}^\lambda$  is the diagonal matrix element of the  $\hat{Q}_\lambda$  operator and  $v_\nu$  denotes the particle occupation factor in the single particle state  $|\nu\rangle$ . The summation goes over proton states. The mean square radii of nuclei  $\langle r^2 \rangle^A$  are related to the electric monopole moments  $Q_0$ :

$$\langle r^2 \rangle^A = \frac{Q_0}{Z}. \quad (6)$$

They usually are not given in experiment straight, we deal rather with the isotopic shifts of  $\langle r^2 \rangle$  between various mass numbers:

$$\delta \langle r^2 \rangle^{A,A'} = \langle r^2 \rangle^A - \langle r^2 \rangle^{A'}. \quad (7)$$

To present the growth of nuclear square radii with neutron number we choose an average number  $A'$  for every element and give the relative value  $\delta \langle r^2 \rangle^{A,A'}$ , because the absolute values are model dependent.

### 3. Results

At first we have studied the influence of the quadrupole pairing interaction on the potential energy surface. It is interesting to look at the behaviour of the energy around the equilibrium deformation. In Figs 1 and 2 the potential energy surfaces for two nuclei from the investigated region are shown in the  $(\epsilon_2, \epsilon_4)$  plane. One can see that the energy surface is very flat and hence finding of the equilibrium deformation of the nucleus is very difficult.

In Table I we show the equilibrium deformations of Sr isotopes calculated for monopole pairing interaction and with both kinds of pairing forces (in the Table signed as monopole + quadrupole pairing). By  $E_{\text{tot}}$  we denote the Strutinsky energy at equilibrium deformation.

TABLE I

Equilibrium deformations of Sr isotopes.

Z	N	monopole pairing			monopole+quadrupole pairing		
		$\epsilon_2$	$\epsilon_4$	$E_{\text{tot}}$ MeV	$\epsilon_2$	$\epsilon_4$	$E_{\text{tot}}$ MeV
38	38	0.381	0.034	-0.62666	0.410	0.070	-0.80850
38	40	0.378	0.054	0.06674	0.350	0.050	-0.62001
38	42	-0.250	0.040	0.53533	-0.250	0.010	-1.57588
38	44	-0.250	0.040	0.00151	-0.225	0.020	-2.81227
38	46	0.050	0.000	-1.17164	-0.100	0.020	-4.09453
38	48	0.000	0.000	-3.68367	-0.050	0.010	-5.44648
38	50	0.025	0.000	-7.51131	0.000	0.000	-8.63073
38	52	0.000	0.000	-4.07740	-0.030	0.010	-5.25056
38	54	0.050	0.000	-1.70948	0.050	0.010	-2.83149
38	56	0.175	0.000	0.16746	0.150	0.010	-0.71126
38	58	0.300	0.000	0.61351	0.270	0.020	0.32051
38	60	0.313	-0.003	0.17349	0.317	0.047	-1.23982
38	62	0.325	0.010	0.24106	0.313	0.052	-0.44848
38	64	0.330	0.026	0.33581	0.321	0.010	0.13393
38	66	0.375	0.020	0.02300	0.400	0.060	-0.13032
38	68	0.375	0.030	-0.56592	0.400	0.060	-0.49309
38	70	0.382	0.052	-1.77134	0.400	0.050	-1.82441
38	72	0.375	0.075	-1.15501	0.400	0.070	-3.04713
38	74	0.300	0.040	-0.03279	0.400	0.070	-0.35608

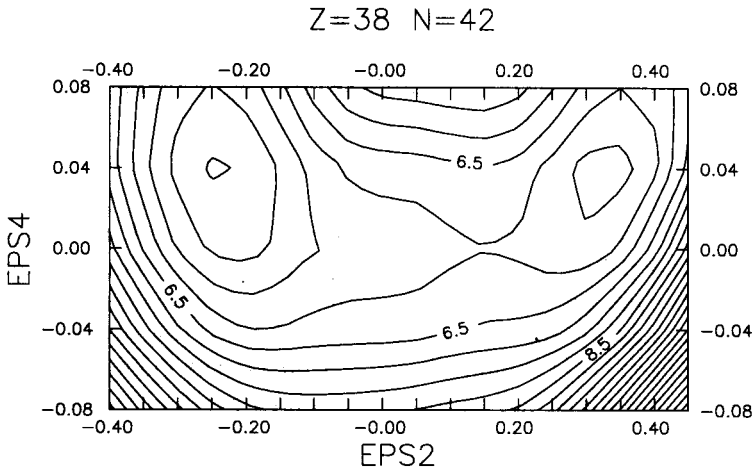


Fig. 1. Contour map of the potential energy  $V$ , plotted as a function of the quadrupole  $\epsilon_2$  (on figure denoted as EPS2) and hexadecapole  $\epsilon_4$  (EPS4) deformation parameters for  $^{80}\text{Sr}$ .

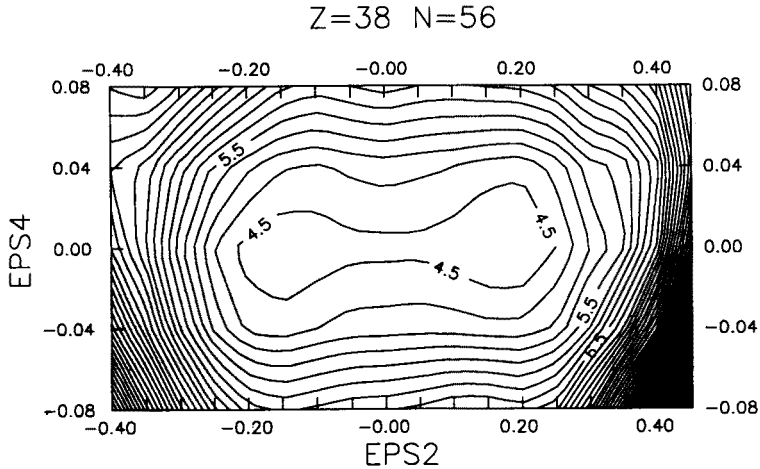


Fig. 2. The same as in Fig. 1 for  $^{94}\text{Sr}$ .

In general, for all the investigated nuclei the quadrupole pairing interaction does not change equilibrium deformations significantly but the total energy becomes 1–2 MeV smaller. Only for a few nuclei the differences in equilibrium deformations between the two kinds of calculations are large (for example the prolate equilibrium shapes for monopole pairing forces and oblate for quadrupole pairing in  $^{82}\text{Sr}$ ).

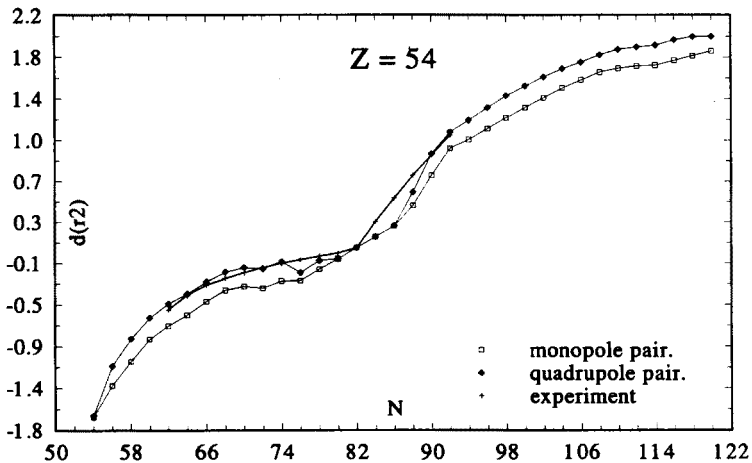


Fig. 3. Charge mean square radius isotope shifts  $\delta \langle r^2 \rangle^{A,A'}$  of Xe isotopes in  $\text{fm}^2$  related to the  $A'$  mass number corresponding to the magic neutron number  $N = 82$  ( $A' = N + Z$ ). Solid diamonds denote theory with the monopole and quadrupole pairing forces, empty boxes — with the monopole pairing interaction and crosses — the experimental data.

In Figs 3–8 the isotopic shifts of the mean square radii  $\delta\langle r^2 \rangle$  for a few nuclei of the considered region are shown. They were calculated in two cases: with the monopole and quadrupole pairing forces (solid diamonds on figures) and with monopole pairing interactions only (empty boxes). The crosses denote the experimental values. It is seen that the isotopic shifts  $\delta\langle r^2 \rangle$  calculated with the quadrupole pairing forces lie closer to the experimental data than those obtained with the monopole pairing interaction only. The kink effect in the experimental data (starting at  $N = 82$ ) is better reproduced too, when including the quadrupole pairing interaction.

Presented in Fig. 9 the isotopic shift of the mean square radius for Sr isotopes calculated in the two dimensional deformation space  $\{\epsilon_\lambda\} = \epsilon_2, \epsilon_4$ ,

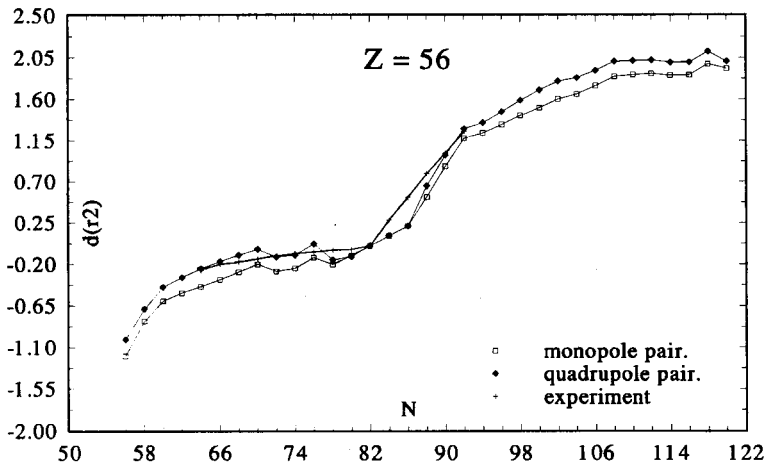


Fig. 4. The same as in Fig. 3 for Ba isotopes.

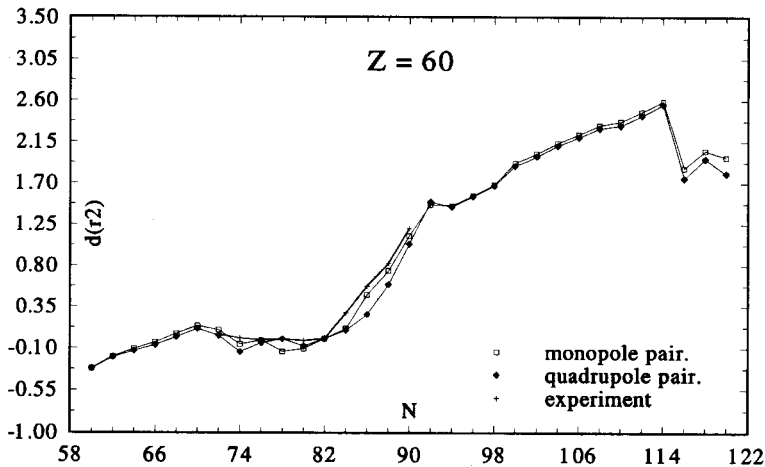


Fig. 5. The same as in Fig. 3 for Nd isotopes.

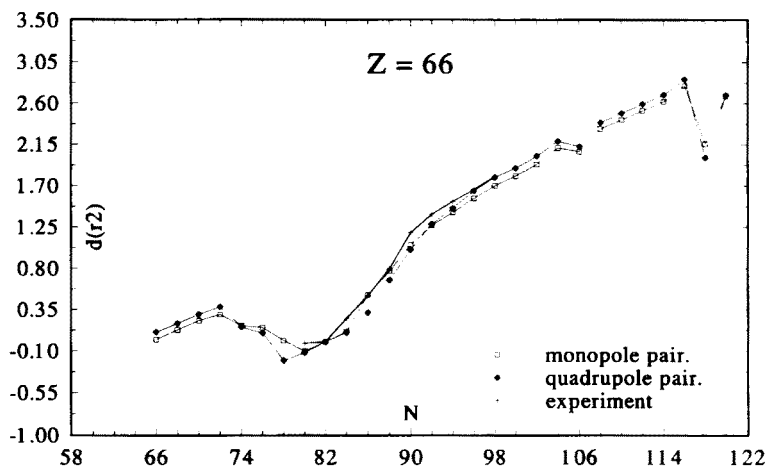


Fig. 6. The same as in Fig. 3 for Dy isotopes.

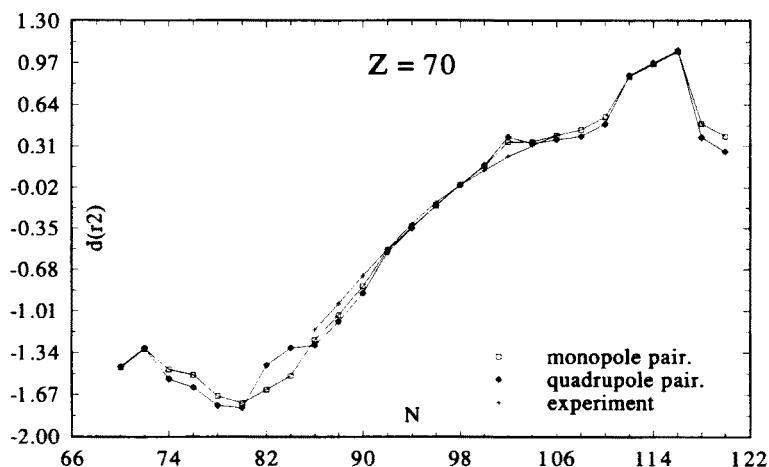


Fig. 7. The same as in Fig. 3 for Yb isotopes.

with quadrupole pairing forces (diamonds) and without it (boxes) does not reproduce well the experimental data. In order to improve the results we analysed their dependence on higher order deformations. The potential energy was analysed in the five-dimensional deformation space  $\{\epsilon_\lambda\}$ ,  $\lambda = 2, 3, 4, 5, 6$ . The equilibrium of deformation of a nucleus was found by minimizing its ground-state potential energy in the five deformation parameters simultaneously:  $\epsilon_2, \epsilon_3, \epsilon_4, \epsilon_5, \epsilon_6$ , all treated as independent variables. To minimize the energy in the full space  $\{\epsilon_\lambda\}$ , the numerical procedure ZXMIN of the IMSL library was used.

Fig. 10 shows the isotopic shifts of the  $m_{sr}$  for Sr isotopes calculated

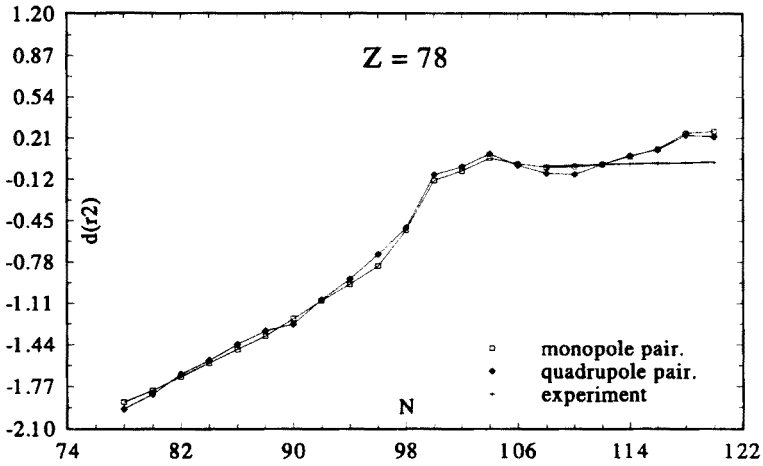


Fig. 8. The same as in Fig. 3 for Pt isotopes.

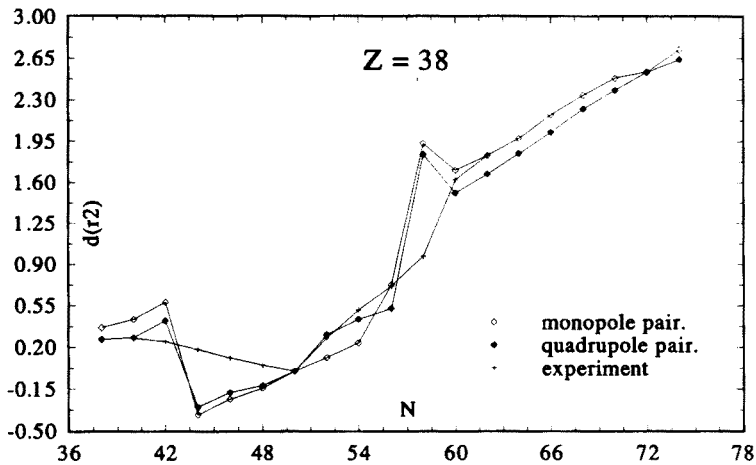


Fig. 9. Charge mean square radius isotope shifts  $\delta \langle r^2 \rangle^{A, A'}$  of Sr isotopes in  $\text{fm}^2$  related to the  $A' = 88$ ,  $\langle r^2 \rangle^{A'}$  analysed in two-dimensional deformation space. The symbols are the same as in previous figures.

in five-dimensional deformation space  $\{\epsilon_\lambda\} = \epsilon_2, \epsilon_3, \epsilon_4, \epsilon_5, \epsilon_6$ . It is seen that these results calculations in five dimensional deformation space reproduce a little bit better experimental points than those obtained in the two dimensional only (Fig. 9).

It is well known that the results of calculations depend on the strengths of pairing interactions, especially on the strength of the quadrupole pairing forces which was chosen rather arbitrarily [12]. For the purpose of investigation of the dependence of the msr on the pairing strengths we made



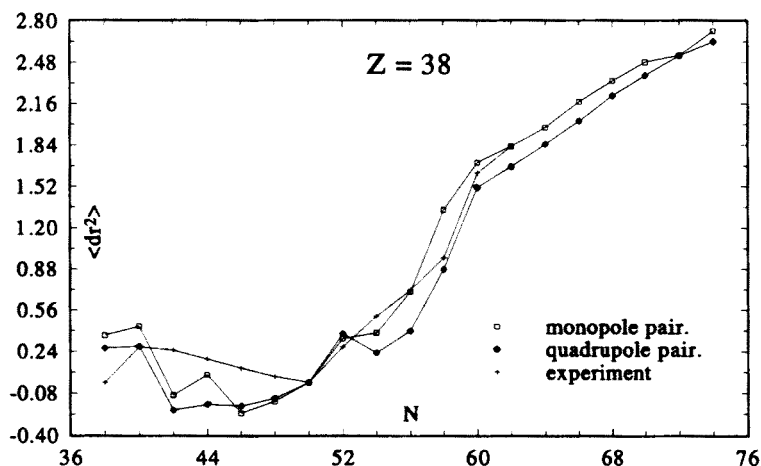


Fig. 10. The same as in Fig. 9 analysed in five-dimensional deformation space.

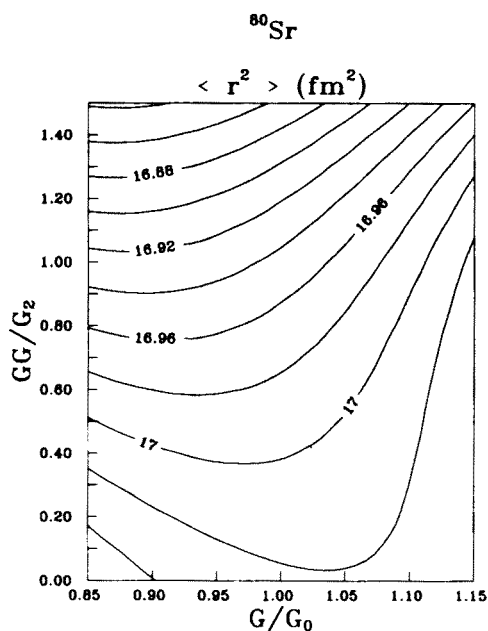


Fig. 11. Mean square radii  $\langle r^2 \rangle$ , plotted as a function of the strength of the monopole  $G$ , and quadrupole  $GG$  pairing forces (on the figure have been given the relative value  $G/G_0$  and  $GG/G_2$ , where  $G_0$  and  $G_2$  are their standard values).

calculations for various values of  $G_0$  and  $G_2$ . The pairing strengths were changed in the ranges:

$$\begin{aligned} 0.85 * G_0 \leq G \leq 1.15 * G_0, \\ 0 \leq GG \leq 1.5 * G_2. \end{aligned} \quad (8)$$

Here  $G$  and  $GG$  are the strengths of the monopole and quadrupole pairing forces, whereas  $G_0$  and  $G_2$  are their standard values. The results of calculations of  $^{80}\text{Sr}$  isotope are shown in Fig. 11. The points of the equal  $\langle r^2 \rangle$  are joined by solid lines and signed by values in  $\text{fm}^2$ . It is seen that the increase of the value of the quadrupole pairing strength from zero (that means excluding of the quadrupole pairing forces) to  $1.5 * G_2$  (the quadrupole pairing 50% stronger) gives the difference in  $\langle r^2 \rangle$  only  $\sim 0.12 \text{ fm}^2$ . This value is too small in order to explain the discrepancy between results of our calculations and experimental data ( $\sim 0.25 \text{ fm}^2$  for this nucleus) for any  $G_2$  value. A similar situation is obtained for other nuclei. The remaining discrepancy in  $\delta\langle r^2 \rangle$  between our model and experiment is probably due to some shell effects not properly described by our single particle potential *e.g.* the negligence of the nonaxial deformation.

#### 4. Conclusions

The following conclusions can be drawn from our investigation:

- (i) For many nuclei the difference in energy between the oblate and prolate minimum is small and the energy surface around the equilibrium deformation is very flat.
- (ii) Generally the isotopic shifts  $\delta\langle r^2 \rangle^{A,A'}$ , calculated with the quadrupole pairing forces, lie closer to the experimental data than those obtained with the monopole pairing interaction only.
- (iii) The mean square radii of nuclei depend on the dimension of deformation space.
- (iv) The quadrupole pairing forces explain only partly the discrepancy between theory and experiment.

#### REFERENCES

- [1] E.W. Otten, *Treatise on Heavy Ion Science*, Vol. 8, Ed. D. Allan Browley, Plenum Publishing Corporation, 1984, p.517.
- [2] P. Aufmuth, K. Heiling, A. Steudel, *Atomic Data and Nucl. Data Tables*, Vol. 37, 1985, p.455.
- [3] S. Raman, C.H. Malankey, W.T. Milner, C.W. Nestor jr., P.H. Stelson, *Atomic Data and Nucl. Data Tables*, Vol. 36, 1987, p.1.
- [4] H. Mach *et al.*, *Nucl. Phys.* **A523**, 197 (1991).

- [5] B. Nerlo-Pomorska, *Nucl. Phys.* **A259**, 481 (1976).
- [6] P. Rozmej, *Nucl. Phys.* **A445**, 495 (1985).
- [7] B. Nerlo-Pomorska, K. Pomorski, *Annales Univ. MCS, Sec. AAA, Lublin, Poland XLIII/XLIV*, 21 (1988/1989).
- [8] B. Nerlo-Pomorska, K. Pomorski, B. Skorupska, Proc. XXI Masurian School on Nuclear Physics, 26 August–5 September, 1990.
- [9] B. Nerlo-Pomorska, B. Skorupska, *Annales Univ. MCS, Sec. AAA, Lublin, Poland XLV*, 10, 90 (1990).
- [10] T. Seo, *Z. Phys.* **A324**, 43 (1986).
- [11] B. Nerlo-Pomorska, K. Pomorski, B. Skorupska-Mach, *Nucl. Phys.* **A562**, 180 (1993).
- [12] S.G. Nilsson, J.R. Nix, P. Möller, I. Ragnarsson, *Nucl. Phys.* **A222**, 221 (1974).
- [13] V.M. Strutinsky, *Nucl. Phys.* **A95**, 420 (1967); *Nucl. Phys.* **A122**, 1 (1968).
- [14] V. Myers, W.J. Swiatecki, *Ann. Phys.* **55**, 395 (1969).